Bioactive Materials 4 (2019) 97–106

Contents lists available at ScienceDirect

Bioactive Materials

journal homepage: http://www.keaipublishing.com/biomat

# Viable cryopreserved umbilical tissue (vCUT) reduces post-operative adhesions in a rabbit abdominal adhesion model

Sandeep Dhall[a,*], Turhan Coksaygan[b], Tyler Hoffman[a], Matthew Moorman[a], Anne Lerch[a], Jin-Qiang Kuang[a], Malathi Sathyamoorthy[a], Alla Danilkovitch[a]

[a] Osiris Therapeutics, Inc., 7015 Albert Einstein Dr, Columbia, MD, 21046, USA
[b] University of Maryland, 655 W. Baltimore Street, Baltimore, MD, 21201, USA

ARTICLE INFO

*Keywords:*
Placental
Cryopreserved
Post-surgical
Adhesiolysis
Inflammation
Fibrosis

ABSTRACT

Post-operative adhesions, a common complication of surgery, cause pain, impair organ functionality, and often require additional surgical interventions. Control of inflammation, protection of injured tissue, and rapid tissue repair are critical for adhesion prevention. Adhesion barriers are biomaterials used to prevent adhesions by physical separation of opposing injured tissues. Current adhesion barriers have poor anti-inflammatory and tissue regenerative properties. Umbilical cord tissue (UT), a part of the placenta, is inherently soft, conforming, biocompatible, and biodegradable, with antimicrobial, anti-inflammatory, and antifibrotic properties, making it an attractive alternative to currently available adhesion barriers. While use of fresh tissue is preferable, availability and short storage time limit its clinical use. A viable cryopreserved UT (vCUT) "point of care" allograft has recently become available. vCUT retains the extracellular matrix, growth factors, and native viable cells with the added advantage of a long shelf life at −80 °C. In this study, vCUT's anti-adhesion property was evaluated in a rabbit abdominal adhesion model. The cecum was abraded on two opposing sides, and vCUT was sutured to the abdominal wall on the treatment side; whereas the contralateral side of the abdomen served as an internal untreated control. Gross and histological evaluation was performed at 7, 28, and 67 days post-surgery. No adhesions were detectable on the vCUT treated side at all time points. Histological scores for adhesion, inflammation, and fibrosis were lower on the vCUT treated side as compared to the control side. In conclusion, the data supports the use of vCUT as an adhesion barrier in surgical procedures.

## 1. Introduction

Post-operative adhesions are a common complication of surgical procedures. An estimated 90% of patients after gynecologic surgeries and 93%–100% and 67%–93% of patients undergoing upper and lower abdominal laparotomies, respectively, develop post-operative adhesions [1–3]. Approximately, half of all readmitted patients suffer from post-surgical adhesions and require adhesiolysis surgery. However, adhesions often reoccur irrespective of the type of adhesiolysis procedure or characteristics of the initial adhesions [3]. In the US, post-surgical adhesions account for an estimated 303,836 hospitalizations for adhesiolysis, corresponding to 846,415 days of inpatient care and $1.3 billion in annual hospital and surgical care costs [4,5].

Sustained inflammation, increased exudate and fibrin deposition, decreased fibrinolysis, and delayed tissue healing at a surgical site may lead to adhesion formation between injured tissues [6,7]. Adhesion

*Abbreviation list:* Ang, angiogenin; ANGPT1, angiopoietin-1; ANGPT2, angiopoietin-2; ASTM, American Society for Testing and Materials; bFGF, basic fibroblast growth factor; C, Celsius; cAM, calcein acetoxymethyl; cm, centimeter; $CO_2$, carbon dioxide; DMEM, Dulbecco's modified Eagle's medium; DMSO, dimethyl sulfoxide; DPBS, Dulbecco's phosphate-buffered saline; EGF, epidermal growth factor; ECM, extracellular matrix; EtHd-1, ethidium homodimer-1; FBS, fetal bovine serum; FDA, United States Food & Drug Administration; H&E, hematoxylin and eosin; HGF, hepatocyte growth factor; HRP, horseradish peroxidase; iNOS, inducible nitric oxide synthase; CD, cluster of differentiation; DAB, 3,3′-Diaminobenzidine; IgG, immunoglobulin; IGFBP-1, insulin-like growth factor binding protein-1; IL-10, interleukin 10; IL-1RA, interleukin-1 receptor antagonist; MT, Masson's trichrome; mg/kg, milligram/kilogram; IV, intravenous; mm, millimeter; PBS, phosphate-buffered saline; PDGF-AA, platelet-derived growth factor AA; PDGF-BB, platelet-derived growth factor BB; PLGA, poly(lactic-co-glycolic acid); PLGF, placental growth factor; rpm, revolutions per minute; SD, standard deviation; SDF-1α, stromal cell-derived factor 1 alpha; TIMP-1, tissue inhibitor of metalloproteinases-1; UT, umbilical cord tissue; VEGF-D, vascular endothelial growth factor-D; vCUT, viable cryopreserved umbilical tissue

Peer review under responsibility of KeAi Communications Co., Ltd.

* Corresponding author.
*E-mail address:* sdhall@osiris.com (S. Dhall).

https://doi.org/10.1016/j.bioactmat.2018.09.002
Received 3 July 2018; Received in revised form 18 September 2018; Accepted 26 September 2018
Available online 10 October 2018

barriers are biomaterials that are commonly applied at a surgical site to physically separate injured tissues [8]. Synthetic grafts that serve as a physical barrier separating the opposing tissues are commonly used to prevent adhesions [8,9]. Most recently several sprayable/liquid adhesion barriers have been developed. Such sprays are easier to apply, they are adhering and conforming to irregular and complex surfaces [10,11]. An ideal adhesion barrier would be biocompatible, nonimmunogenic, anti-inflammatory, biodegradable, with a degradation rate synchronized with tissue healing, and biomechanically strong for ease of application. Currently, there are no biomaterials that possess all these desired characteristics [8]. The search for ideal biomaterials to prevent post-surgical adhesions is an ongoing effort.

Umbilical cord tissue (UT) is comprised of umbilical amnion and Wharton's jelly [12]. UT is biocompatible, biodegradable, and non-immunogenic, and has inherent anti-inflammatory, antifibrotic, antimicrobial, analgesic, and angiogenic properties [12–14]. These properties are attributed to UT's 3-dimensional collagen and hyaluronic acid-rich extracellular matrix, its native cocktail of cytokines and growth factors, and tissue resident viable cells, including mesenchymal stem cells [15–18]. Furthermore, UT is soft, conforming, and can be sutured. The thickness, handling, and biomechanical properties make UT a suitable graft for surgical applications. However, the use of fresh UT tissue is limited by its short storage time. Advances in cryopreservation have allowed the development of viable cryopreserved umbilical cord tissue (vCUT), which retains all the characteristics of fresh tissue with the advantage of long-term storage. vCUT is an “off-the-shelf” point-of-care commercial placental tissue allograft that is currently being used clinically in the management of limb-salvage cases and tendon and fistula surgical repairs [19–21]. The ease of surgical application, in conjunction with the demonstrated inherent properties of vCUT, prompted this study to further evaluate the use of vCUT for the prevention of post-surgical adhesion in a rabbit abdominal adhesion model.

## 2. Research design and methods

### 2.1. Tissue procurement and ethics statement

Human, normal, full-term placentas were provided by the National Disease Research Interchange (Philadelphia, PA) and Cord Blood America, Inc. (Las Vegas, NV) from eligible donors after obtaining written informed consent. Tissue procurement and ethics statement were provided by The National Disease Research Interchange and Cord Blood America, Inc.

### 2.2. vCUT processing

Placental tissues were aseptically processed in a biological safety cabinet within 36 h after collection. The human UT was separated from the amnion, chorion, and decidua by blunt dissection. The UT was cut to expose the blood vessels and all vessels were removed using blades and forceps, washed with saline, and mechanically cleaned to remove residual blood. The UT was then incubated in Dulbecco's modified Eagle's medium (DMEM) (GE Healthcare Life Sciences, Piscataway, NJ) containing an antibiotic cocktail of gentamicin (Fresenius Kabi, Lake Zurich, IL), vancomycin (Hospira, San Jose, CA), and amphotericin B (Sigma-Aldrich, St. Louis, MO) for 18–48 h at 37 °C and 5% $CO_2$ in a humidified atmosphere. Residual antibiotics were removed by washing with Dulbecco's phosphate-buffered saline (DPBS) (Life Technologies, Carlsbad, CA), and the UT was cut into 5 $cm^2$ pieces. Cryopreservation of UT was performed by freezing UT in a bag with a dimethyl sulfoxide (DMSO) (Mylan Inc., Canonsburg, PA) containing cryoprotectant solution at a controlled 0.4 °C/minute cooling rate established with a temperature probe. Viable cryopreserved UT (vCUT) was stored at −80 °C prior to the experiments.

### 2.3. vCUT thawing procedure

Viable cryopreserved UT was thawed by placing the frozen bag in a water bath at 37 °C for 5–15 min and immediately transferred into a basin with sterile phosphate-buffered saline (PBS).

### 2.4. Assessment of vCUT cell viability

Umbilical tissues from 6 donors were used for all experiments assessing cell viability of the tissue. LIVE/DEAD viability/cytotoxicity kit (Life Technologies, Carlsbad, CA) was used following manufacturer's instructions. Briefly, samples were incubated in a 1:1000 dilution of calcein acetoxymethyl (cAM) and ethidium homodimer-1(EtHd-1) for 30 min and analyzed using a fluorescent microscope (Eclipse TE300; Nikon). Viable cells within the tissue were identified by green fluorescent cAM staining, whereas dead cells were stained with red fluorescent EtHd-1. Images acquired in green and red channels were merged using ImageJ (National Institute of Health, Bethesda, MD).

Outgrowth of cells from vCUT explants was used to confirm the presence of viable cells within the tissue. Thawed vCUT was cauterized onto a 10 cm Petri dish and incubated in DMEM with 10% fetal bovine serum (FBS) (Life Technologies, Carlsbad, CA) and 1 × antibiotic-antimycotic (Life Technologies, Carlsbad, CA) for 7–14 days. Outgrowth of cells from vCUT onto the Petri dish was analyzed microscopically, and images were taken with an Olympus IX70 inverted microscope equipped with a digital camera (Olympus, Waltham, MA).

Fresh UT samples, from the same donors as vCUT, were used as a positive control for cell viability and cell outgrowth assessments.

### 2.5. Detection of growth factors and cytokines present in vCUT

Umbilical tissue from 6 donors was used for evaluation of growth factor and cytokine profiles. Five $cm^2$ samples of fresh UT and vCUT were prepared from placentas derived from the same donors. The vCUT was thawed prior to experiments as described under “vCUT thawing procedure”. Tissue extracts were prepared by homogenizing fresh UT, or vCUT in a T-PER buffer (Thermo Fisher Scientific, Waltham, MA) supplemented with a protease inhibitor cocktail (Sigma, St. Louis, MO) using a gentleMACS Dissociator (Miltenyi Biotec, Auburn, CA). Tissue extracts were clarified by centrifugation (Eppendorf, Hauppauge, NY) at 14,000 revolutions per minute (rpm) for 15 min. Clarified tissue extracts were analyzed using a multiplex growth factor panel kit (LXSAHM-15, R&D Systems, Minneapolis, MN) and Bio-Plex MAGPIX (Bio-Rad, Hercules, CA). The test panel included interleukin 10 (IL-10), interleukin-1 receptor antagonist (IL-1RA), platelet-derived growth factor BB (PDGF-BB), basic fibroblast growth factor (bFGF), stromal cell-derived factor 1 alpha (SDF-1α), angiopoietin-1 (ANGPT1), angiogenin (Ang), angiopoietin-2 (ANGPT2), epidermal growth factor (EGF), hepatocyte growth factor (HGF), tissue inhibitor of metalloproteinases-1 (TIMP-1), insulin-like growth factor binding protein-1 (IGFBP-1), vascular endothelial growth factor-D (VEGF-D), platelet-derived growth factor AA (PDGF-AA), and placental growth factor (PIGF).

### 2.6. Evaluation of biomechanical properties

Biomechanical testing was performed by Community Tissue Services (Dayton, OH). For uniaxial tension and suture retention, nine (n = 9), vCUT strips in the parallel and perpendicular directions from 4 grafts were obtained. For the ball burst test, nine (n = 9), specimens from 7 grafts were selected without regard to fiber direction.

#### 2.6.1. Uniaxial tension testing to failure

A gage length of 27 mm was set for all samples, and 3 thickness measurements within this gage length were obtained using the laser micrometer. All samples were tested at a displacement controlled rate

of 5 mm/s. Load and displacement data were recorded by the material testing system's (ElectroPuls E3000; Instron, Norwood, MA) 100 N load cell (Instron 2530-427, Instron, Norwood, MA) and integrated actuator position sensor, respectively. Maximum stress was calculated as the maximum load divided by the average cross-sectional area for each specimen. Strain at maximum stress was the displacement value corresponding to the maximum stress value divided by the gage length. Stiffness was taken as the slope of a linear regression of the points on the respective diagram.

#### 2.6.2. Suture retention

Suture retention specimens (2 cm × 4 cm) were tested with both parallel and perpendicular oriented fibers. The specimens were clamped in the pneumatic grips with a 2.0 cm tab hanging from the top clamp. A 25.4 cm long segment of wire was placed through the tab 1.0 cm away from the free end, centered in the width of the specimen. The wire was secured to the base of the materials testing system with a custom grip base and post system. The wire was wrapped around a post and twisted around itself in such a way that it would not unwind with the extension of crosshead. The specimen was pulled at a displacement controlled rate of 25.4 mm/s. Load and displacement data were recorded by the material testing system's (ElectroPuls E3000; Instron, Norwood, MA) 100 N load cell (Instron 2530-427, Instron, Norwood, MA) and integrated Linear Variable Differential Transformer (LVDT) position sensor, respectively.

#### 2.6.3. Ball burst test

An average of 3 thickness measurements obtained in each fiber direction using the laser micrometer was calculated. Each specimen was then “sandwiched” between two 220 grit sandpaper rings and clamped between the plates of the ball burst fixture. Tests were conducted at a displacement rate of 305 mm/min, per American Society for Testing and Materials.

(ASTM) Standard D6797 – 021. Load and displacement data were recorded by the material testing system's (ElectroPuls E3000; Instron, Norwood, MA) 100 N load cell (Instron 2530-427, Instron, Norwood, MA) and integrated LVDT position sensor, respectively. Displacement was defined as the indenter travel perpendicular to the plane of the umbilical tissue, with zero located on the specimen's top surface.

### 2.7. Animals

New Zealand White rabbits (Charles River, Inc., Wilmington, MA) were housed at the Noble Life Sciences vivarium in Sykesville, MD. All experimental protocols were approved by the Noble Life Sciences' Institutional Animal Care and Use Committee. All rabbits were fed Harlan Teklad Global High Fiber Rabbit Diet #2031 (Harlan, Madison, WI) *ad libitum*.

### 2.8. Rabbit abdominal adhesion model

Prior to surgery, the rabbits were anesthetized with ketamine (20–40 mg/kg) and xylazine (4–6 mg/kg). Additionally, buprenorphine (0.02–0.05 mg/kg) was administered by an intravenous (IV) catheter in a marginal ear vein and an endotracheal tube was placed. Hair was removed from the rabbit's abdomen using Nair (Church & Dwight Co., Inc., Ewing, NJ). During surgery, the rabbit was maintained under anesthesia with 1%–3% isoflurane + 1–2 Lt $O_2$. Fluid was provided as a 10 mL/kg/h saline IV infusion. A pulse oximeter was used to monitor heart rate and oxygenation. Temperature was monitored every 15 min. Prior to initiation of the procedure, the surgical field was aseptically scrubbed with Nolvasan scrub solution (Zoetis Services LLC, Parsippany, NJ) and rinsed with 70% ethanol. A 10 cm midline laparotomy was made, and the cecum and bowel exposed. The surface of the cecum adjacent to the sidewall defect was abraded with sterile gauze for 15 min until petechial hemorrhage was observed. The surface of the cecum facing the rest of the bowel was abraded for 5 min. Saline was applied to the bowel and serosa to prevent drying. A 3 × 3 cm square of the peritoneum and the abdominal transverse muscle was removed from the right lateral abdominal wall. Each animal had 2 surgical sites; at one site, vCUT was sutured to the injured abdominal wall, whereas the other site served as an internal control. At the end of the surgery, the bowel was placed back into the abdominal cavity, and the muscle wall of the rabbit was closed with intracutaneous running suture (Safil, B. Braun, Bethlehem, PA). The skin was then closed with intracutaneous running suture or skin adhesive surgical glue. Following recovery from anesthesia, long-term post-operative care was performed twice daily for at least 10 days following surgery. Seven, 28, and 67 days post-surgery, animals were euthanized via an IV overdose of sodium pentobarbital while under ketamine/xylazine anesthesia. Gross evaluation of the surgical sites for the presence of abdominal adhesions and strength of the adhesions was performed. Adhesions were scored according to previously reported scoring system: Score 0 = no adhesions; score 1 = filmy adhesions, adhesions that would separate with gravity; score 2 = stronger adhesions, adhesions easy to separate by blunt dissection; score 3 = strong adhesion, lysis possible but by sharp dissection only; score 4 = very strong adhesions, lysis possible by sharp dissection only (organ strongly attached with severe adhesions and damage of organs hardly preventable) [22]. Tissue samples collected from surgical sites were used for histological analysis.

### 2.9. Histological evaluation

Fresh UT, vCUT, and animal tissue samples collected from surgical sites were fixed in 10% formalin for 24 h and then transferred to ethanol. Samples were embedded in paraffin, sectioned at 5 μm, and stained with hematoxylin and eosin (H&E), hyaluronan binding protein (HABP) (Abcam #ab176959, Cambridge, MA), Masson's trichrome (MT) stain, CD68 (Abcam #955, Cambridge, MA), inducible nitric oxide synthase (iNOS) (Abcam #ab3523, Cambridge, MA), and CD163 (Abcam #111250, Cambridge, MA). Heat induced epitope retrieval was performed prior to primary antibody incubation. Rabbit IgG was used as secondary for iNOS.Mouse IgG was used as secondary for CD163 and CD68. DAB was used as the substrate. Standard protocols at Histoserv, Inc. (Germantown, MD) were used to perform staining. Histological scoring of samples was performed by a blinded pathologist at Noble Life Sciences.

### 2.10. Statistical analysis

Results are presented as mean ± standard deviation (SD). Student T-test was used for statistical analysis, and $p < 0.05$ was considered significant.

## 3. Results

### 3.1. Evaluation of structural and cellular integrity of vCUT

Visually, vCUT appears as an ~1–3 mm thick off-white-colored graft (Fig. 1A). Variable thickness across the tissue is mostly due to the presence of grooves after removal of blood vessels. The groove areas are the thinnest area in vCUT (Fig. 1A, labeled by asterisks). Results of biomechanical testing of vCUT are summarized in Fig. 1B. Results are consistent with biomechanical properties of soft connective tissue, including fresh UT as reported in the literature [23–25].

The structural integrity of the extracellular matrix in vCUT was evaluated histologically using hematoxylin and eosin (H&E) staining, and immunohistochemical staining for hyaluronic acid binding protein (HABP). When compared to fresh UT, vCUT showed no changes in tissue architecture (Fig. 1C). The presence of epithelial cells in the umbilical amnion and sparsely distributed stromal cells and fine collagenous fibers in the Wharton's jelly (WJ) were revealed by H&E

A

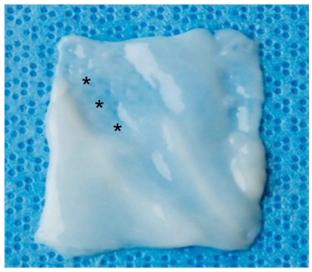

B

| Test* | Tissue Fiber Orientation | Load (N) | Displacement (mm) | Stiffness at max load (N/mm) |
|---|---|---|---|---|
| Suture Retention | Parallel | 3.67 ± 0.95 | 11.56 ± 2.93 | N/A |
| | Perpendicular | 2.62 ± 1.34 | 13.38 ± 6.42 | N/A |
| Uniaxial tensile strength | Parallel | 4.45 ± 1.38 | 11.03 ± 2.47 | 0.43 ± 0.33 |
| | Perpendicular | 5.66 ± 2.19 | 9.45 ± 2.4 | 0.46 ± 0.37 |
| Ball Burst | N/A | 15.60 ± 3.50 | 5.67 ± 1.52 | N/A |

*mean ± SD; mm- millimeter; N- Newton; N/A- Not Applicable

C

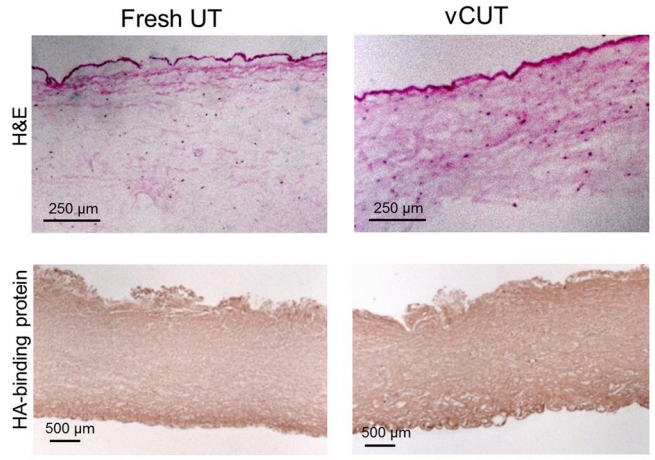


D

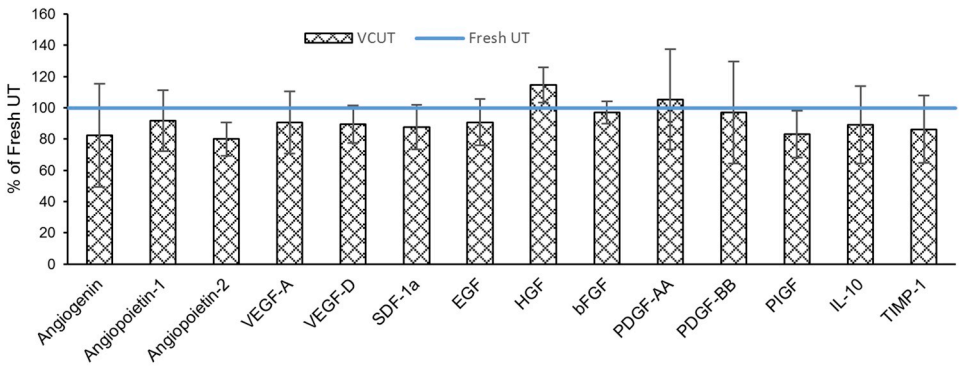


E

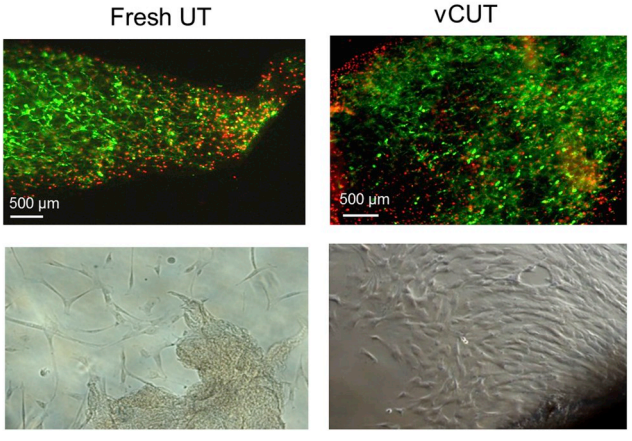


(caption on next page)

**Fig. 1. vCUT characterization. (A)** Visual appearance of vCUT post-thaw. Asterisks show the thinner grooves in the tissue after removal of umbilical blood vessels. **(B)** Biomechanical properties of the vCUT. **(C)** Hematoxylin and Eosin (H&E, top panel) staining and staining with hyaluronan binding protein (HABP)-horseradish peroxidase (HRP) conjugate (bottom panel) of fresh umbilical tissue (UT) (left images) and vCUT (right images). **(D)** Presence of angiogenin (ANG), angiopoietin-1 (ANGPT1), angiopoietin-2 (ANGPT2), vascular endothelial growth factor A (VEGF-A), vascular endothelial growth factor D (VEGF-D), stromal cell derived factor-1α (SDF-1α), epidermal growth factor (EGF), hepatocyte growth factor (HGF), basic fibroblast growth factor (bFGF), platelet derived growth factor AA (PDGF-AA), platelet derived growth factor BB (PDGF-BB), placenta growth factor (PIGF), interleukin 10 (IL-10) and tissue inhibitor of matrix metalloproteinases-1 (TIMP-1) in vCUT. Levels of growth factors are shown in % (mean ± SD) relatively to the levels of corresponding growth factors in fresh UT for 6 donors. **(E)** Cell-viability assessment by staining of fresh UT (top left image) and vCUT post-thaw (top right image) with calcein AM (green-stained viable cells) and ethidium homodimer-1 (red-stained dead cells). Representative images for 1 out of 3 tested donors (bottom panel) show cell outgrowth after placing fresh UT (bottom left image) or vCUT (bottom right image) in culture medium for 10 days.

staining (Fig. 1C *top panel*). There was no difference in hyaluronic acid (HA) amount or its distribution across the tissue between vCUT and fresh UT (Fig. 1C *bottom panel*).

vCUT extracts were assayed to determine the impact of cryopreservation on growth factors that are important for tissue repair and regeneration and compared to levels in fresh UT. No significant difference in levels of EGF, HGF, bFGF, PDGF-AA, PDGF-AA, placenta growth factor (PIGF), ANG, ANGPT1, angiopoietin-2 (ANGPT2), VEGF-A, VEGF-D, SDF-1α, IL-10, and TIMP-1 was found between vCUT and fresh UT (Fig. 1D).

The presence of viable cells in vCUT and fresh UT was demonstrated using the LIVE/DEAD viability/cytotoxicity assay. A qualitative comparison showed that the majority of cells were viable in both vCUT post-thaw and fresh UT (Fig. 1E *top panel)*. Analysis of a large number of stained sections of umbilical tissue showed high variability of cell distribution within the tissue. Viable cells were observed across at least 70% of the tissue. There was no difference in cell viability between fresh and cryopreserved umbilical tissues (Fig. 1E). Furthermore, viability of cells in vCUT post-thaw was confirmed by observed outgrowth of cells that migrated from vCUT and proliferated *in vitro*, similar to fresh UT (Fig. 1E *bottom panel*).

### 3.2. vCUT prevents adhesion in a rabbit model of abdominal adhesion

The study design (Table 1) and a schematic description of the rabbit model of abdominal adhesion, with in-surgery photographs, are shown in Fig. 2. Adhesions in rabbits were induced on both sides of the abdomen. Following abrasion of the cecum (Fig. 2A), a portion of the peritoneum and abdominal transverse muscle was removed (Fig. 2B). vCUT was applied to the injured area and sutured to the abdominal wall (Fig. 2C) at one surgical site. A second surgical site on the same animal did not receive a graft, to serve as an internal control.

Twelve of the 12 (100%) control sites developed adhesions, whereas the sites treated with vCUT showed no adhesions at all time points (Figs. 3–5). By day 7, internal control site had already developed grade 3 adhesions, suggesting that adhesion formation between injured tissues is a very rapid process (Fig. 3A). In contrast, the vCUT treated surgical site did not develop adhesions between the abdominal wall and cecum (Fig. 3B). Histological evaluation showed microscopic morphological changes in the tissue at the internal control site seven days post-surgery. The H&E stained internal control site tissue sections displayed the presence of cecal mucosa, submucosa, and muscularis externa connected to the abdominal wall by fibrous bands (Fig. 3C). The band of fibrous tissue between the cecal layer and abdominal wall was not detected at the vCUT-treated sites. The vCUT graft remained present on the abdominal wall at the surgical site (Fig. 3B and D, fig. S1A). The presence of fibrous bundles of collagen deposition between injured tissues was found in tissue sections from internal control sites via MT staining (Fig. 3E). Collagen deposition was not detected at the vCUT treated sites (Fig. 3F, fig. S1B). To assess inflammation at the surgical site tissue sections collected at day 7 were immunohistochemically stained for CD68 (macrophage marker), iNOS (M1 macrophage marker) or CD163 (M2 macrophage marker). CD68 and CD163-positive cells were detected in neither control nor vCUT-treated tissue sections (Figs. S2A, B, E, F). Both control and vCUT-treated tissue sections had iNOS positive cells (Figs. S2C and D), however these cells were not macrophages as the tissue sections had no CD68-positively stained cells (Figs. S2A and B). Higher abundance of iNOS positive cells were observed in controls than was seen on vCUT treated site. In controls, iNOS distribution was present throughout the cecum and abdominal wall whereas vCUT treatment showed patches of iNOS in the cecum and very little presence in vCUT (Figs. S2A and B).

A second group of animals was evaluated at 28 days post-surgery. Gross visual scoring for the presence and severity of adhesions between abdominal wall and cecum was performed during necropsy (Table 2). Grade 3 adhesions between the cecum and abdominal wall were observed at internal control sites, whereas no adhesions were observed in vCUT treated sites (Fig. 4A and B, and Table 2). At the treated sites, a partial resorption of vCUT graft was observed with the thinner graft remaining on the abdominal wall (Fig. 4B). The presence of fibrosis between abdominal wall and cecum, and abdominal wall and vCUT tissue section were scored by a blinded third-party pathologist (Table 2). The incidence of inflammation was determined by the presence of inflammatory cells (Table 2). A thick layer of grade 3 fibrous tissue between the cecum and abdominal wall present at internal control sites 28 days post-surgery was revealed by H&E staining (Fig. 4C, Table 2). Adhesions were not detected upon histological evaluation in samples from vCUT treated sites (Fig. 4D and fig. S1C). However, lower grade 2 fibrosis between vCUT and the abdominal wall was detected histologically (Fig. S1C, Table 2). Also, a small number of inflammatory cells in the vCUT graft were detected by H&E staining (Fig. 4D, fig. S1C: marked by asterisk, Table 2). Highly unaligned bundles of dense collagen fibers were detected in the region of adhesions in the MT stained internal control site tissue sections (Fig. 4E, arrows). The penetration of collagen fibers into the cecal muscle and abdominal muscle layers was histologically confirmed by the formation of tight adhesions (Fig. 4E, arrows). In vCUT treated sites, no collagen deposition was detected on MT stained tissue sections. vCUT was still present at the site, and it was attached to the abdominal wall with minimal collagen fibers and fibroblast infiltration (Fig. 4F, fig. S1D).

67 days post-surgery, internal control sites had grade 3 adhesions similar to those found on day 7 and 28. (Fig. 5A). Treated surgical sites had no adhesions, with the healed abdominal wall containing remnants of vCUT (Fig. 5B). Histologically, a complete “fusion” between the abdominal wall and cecum was observed for the internal control sites, but not at the vCUT treated sites (Fig. 5C–F). By day 67 post-surgery, the vCUT graft was almost completely resorbed, and both the abdominal wall and cecum were healed normally without attachment to each

**Table 1**
Study design.

| Experimental Group | Time points & number of animals[a] | | | Treatment type applied to each injury site |
|---|---|---|---|---|
| | Day 7 | Day 28 | Day 67 | |
| 1 | 1 | 1 | 1 | Control/Control |
| 2 | 1 | 1 | 1 | vCUT/vCUT |
| 3 | 2 | 2 | 2 | vCUT/Control |

[a] Each animal had two injury sites.

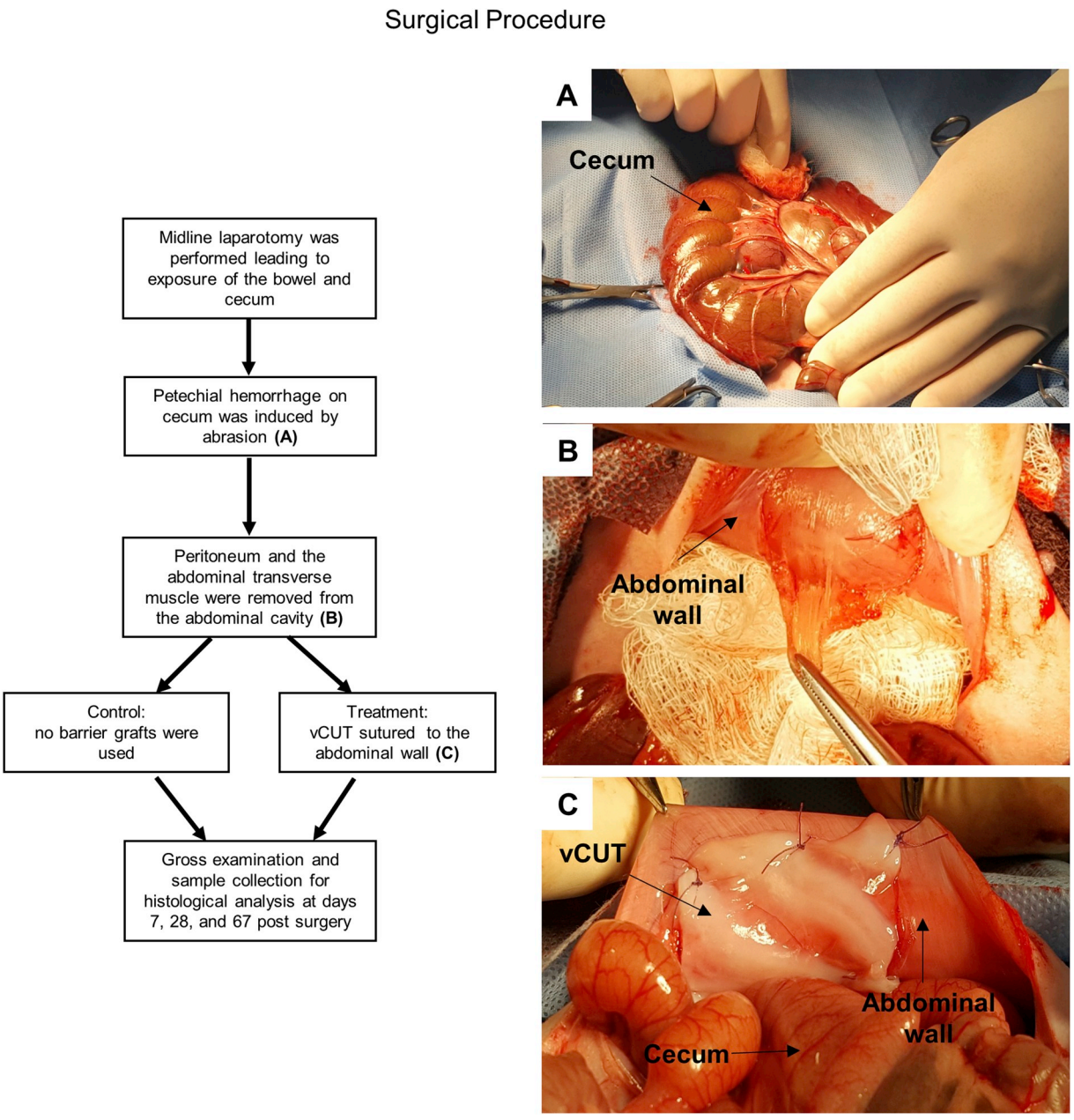


**Fig. 2. Rabbit sidewall defect-cecum abrasion model**. Study design is described in Table 1, and a schematic representation of the surgical procedure is shown to the left of **A-C**. Each animal had two injury sites. Photographs **2A-C** show key steps of the surgical procedure: **(A)** Cecum was abraded for 15 min on one side, resulting in profuse bleeding. The surface of the cecum facing the rest of the bowel was also abraded for 5 min. **(B)** Abdominal wall was abraded by removal of a portion of the abdominal wall muscle layer from the abdominal cavity to induce bleeding and inflammation. **(C)** vCUT was sutured to the injured abdominal wall. No vCUT was used at the control sites. Abdomen was closed.

other (Fig. 5).

The effect of vCUT was also evaluated in a more severe experimental setup (Fig. S3), in which the injured cecum was sutured to the peritoneal wall to force formation of adhesions (Fig. S3D). The study design is presented in Table S1. Due to severity of this experimental setup each animal had only one surgical site. At day 7, animals that had the cecum sutured to the injured abdominal wall developed grade 3 adhesions (Fig. S4A). There were no adhesions present when vCUT was placed between the sutured abdominal wall and cecum (Fig. S4B). Grade 2 adhesions were found only at small areas at the edges of the surgical site where vCUT was not covering the injured tissues (Fig. S4B). Grade 4 adhesions developed in control animals by 28 days post-surgery (Fig. S4C). Similar to day 7, at 28 days post-surgery, grade 2 adhesions were found only in areas where vCUT was not covering injured tissues (Fig. S4D). Lower grade fibrosis and inflammation in the vCUT treated versus control animals was confirmed by histological scoring 28 days post-surgery (Table S2). Similar to day 28, at day 67 post-surgery, grade 4 adhesions were present only in control animals (Figs. S4E and F).

## 4. Discussion

Placental membranes and umbilical cord tissue have anti-inflammatory, anti-oxidant, antifibrotic, and proangiogenic properties that support the natural healing processes of injured tissues [26–30]. However, one of the biggest limitations of fresh tissue is its short storage time. Recent advances in tissue preservation led to the development of commercially available cryopreserved placental tissue that

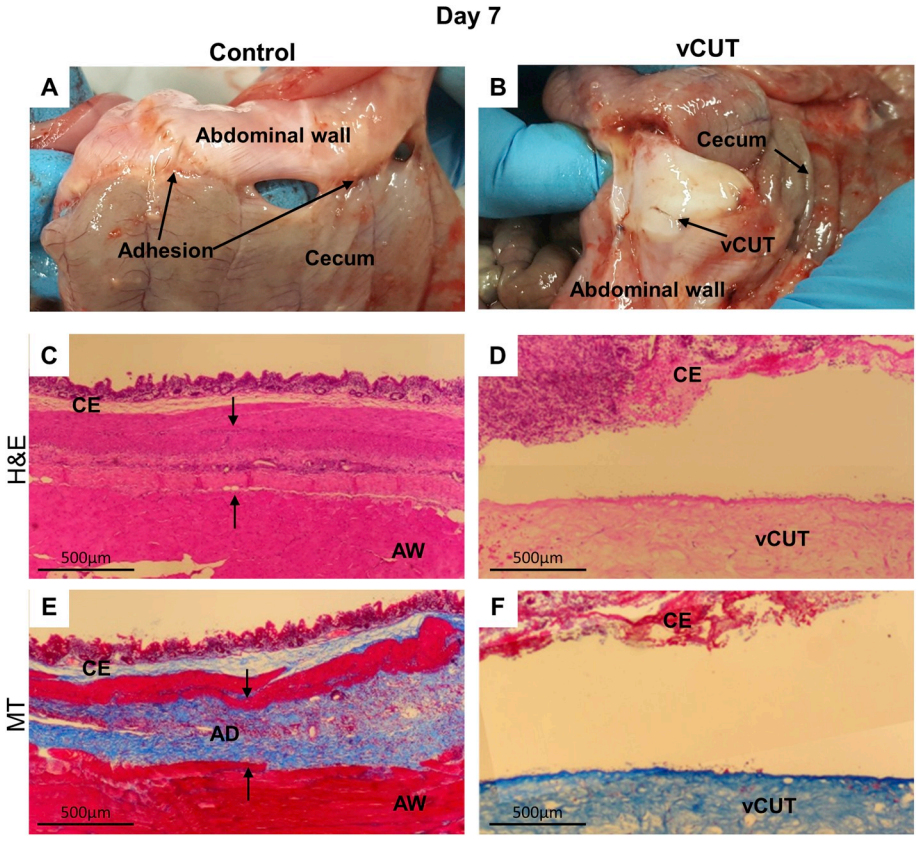


**Fig. 3. Gross and histological evaluation of peritoneal adhesions at day 7 post-surgery. (A)** Abraded abdominal wall directly opposed to the cecum showed early adhesion formation at control sites. Adhesions involved multiple bowel segments. **(B)** In the presence of vCUT, there were detectable adhesions. Localized bleeding was observed at the site as a result of surgical intervention. **(C, D)** H&E-stained tissue sections of control **(C)** and vCUT-treated injury **(D)** sites. Arrows show an adhesion band at the control site. **(E, F)** Masson's trichrome–staining shows the presence of fibrous tissue between the cecum and abdominal wall in control sites **(E)** and no fibrosis present at vCUT-treated sites **(F)**. AD, adhesion; AW, abdominal wall; B, blood; C, cecum; S, suture; vCUT, cryopreserved placental tissue.

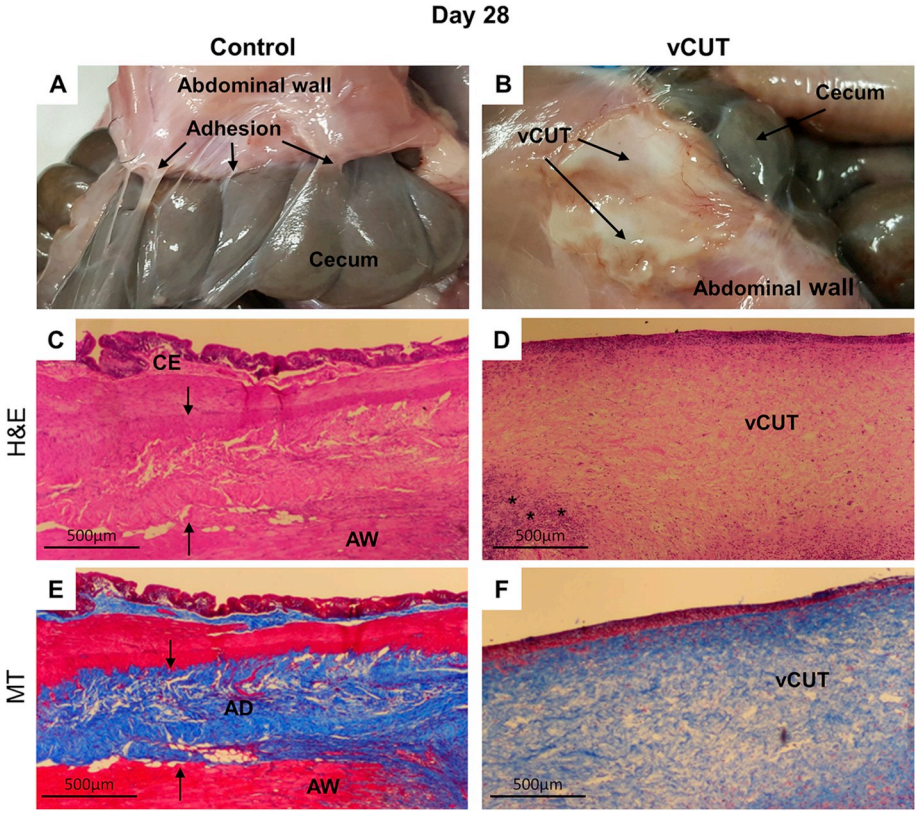


**Fig. 4. Gross and histological evaluation of peritoneal adhesions at day 28 post-surgery.** (**A**) Multiple sections of the cecum have tight adhesions to the abdominal wall. **(B)** In the presence of vCUT, adhesions were not detected. No signs of bleeding at both control and vCUT-treated injury sites. Partially resorbed vCUT was detected at the injury site. **(C, D)** H&E-stained tissue sections of control **(C)** and vCUT-treated injury **(D)** sites. Arrows show an adhesion band at the control site. **(E, F)** Masson's trichrome–staining shows the presence of fibrous tissue between the cecum and abdominal wall at the control site **(E)**, and no fibrosis observed at the vCUT-treated site **(F)**. AD, adhesion; AW, abdominal wall; C, cecum; S, suture; vCUT, cryopreserved placental tissue. Peritoneal adhesion scoring is summarized in Table 2.

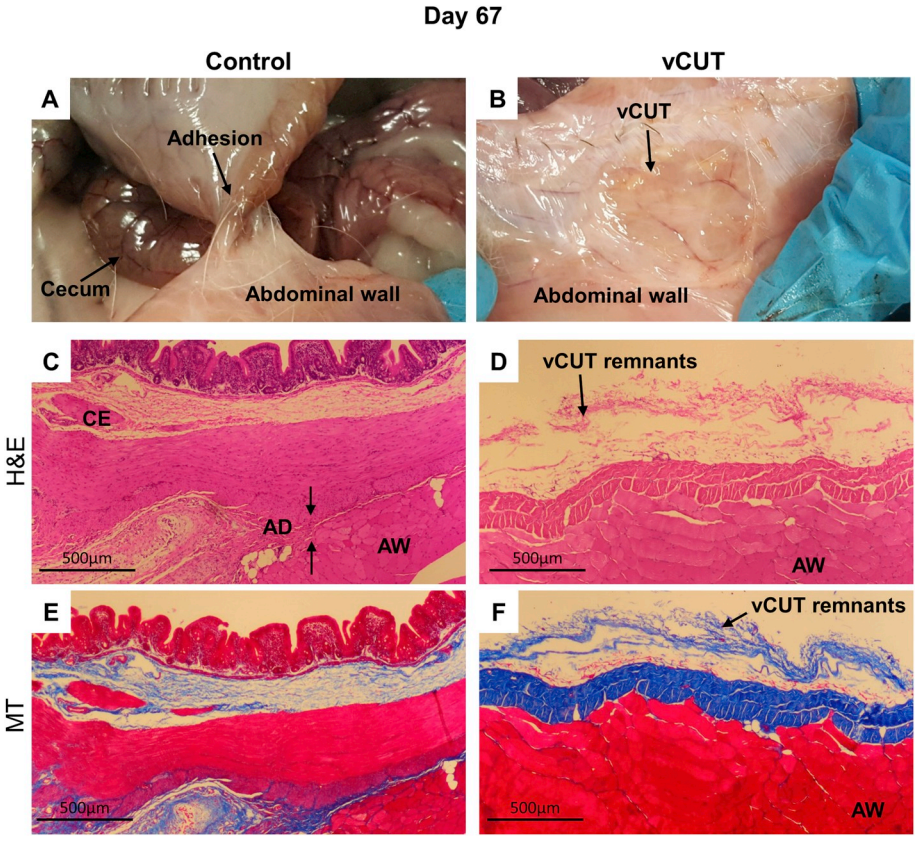


**Fig. 5. Gross and histological evaluation of peritoneal adhesions at day 67 post-surgery. (A)** Sections of the cecum have tight adhesions to the abdominal wall at the control site. **(B)** In the presence of vCUT, adhesions were not detected. Most of vCUT was resorbed with only vCUT residuals visible on the abdominal wall. **(C, D)** H&E-stained tissue sections of control **(C)** and vCUT-treated injury **(D)** sites. Arrows show an adhesion band at the control site. **(E, F)** Masson's trichrome–staining shows the presence of fibrous tissue between the cecum and abdominal wall in control sites. **(E)** No inflammation and fibrosis were observed at the vCUT treated site **(F)**. AD, adhesion; AW, abdominal wall; C, cecum; S, suture; vCUT, cryopreserved placental tissue.

**Table 2**
Peritoneal adhesion scoring.

| Parameters | Score at day 28 | |
|---|---|---|
| | Control | vCUT |
| Adhesion between wall and cecum (gross evaluation) | 3 | 0 |
| Fibrosis (histological evaluation) | 3 | 2[a] |
| Inflammation (histological evaluation) | 3 | 3[a] |

Grading scale: 0 = normal; 1 = minimal; 2 = mild; 3 = moderate; 4 = severe.
[a] Areas between abdominal wall and vCUT with no adhesion to cecum.

retains all native components and properties of fresh tissues, but in contrast to fresh tissue, have long shelf life [31–33].

Results of our characterization studies of vCUT confirm that it retains all the inherent components of the fresh UT. Our studies show that the tissue extracellular matrix (ECM), growth factors, and the endogenous viable cells are all preserved in vCUT (Fig. 1). Both fresh UT and vCUT contain high levels of HA, a natural biopolymer molecule, that possesses anti-inflammatory and antioxidant properties [15,34]. Further, we found that various classes of growth factors native to fresh UT are also present in vCUT (Fig. 1D). Key growth factors-regulators of cellular activities, angiogenic and anti-inflammatory factors that are essential in tissue repair and regeneration were compared in fresh UT and vCUT. Data showed similar levels of growth factors that regulate cell migration, proliferation, and maturation including EGF, HGF, bFGF, PDGF-AA, PDGF-AA, and PIGF. Angiogenic factors of fresh UT such as ANG, ANGPT1, ANGPT2, VEGF-A, VEGF-D, and SDF-1α that promote neovascularization of the damaged tissue are also retained in vCUT. Furthermore, presence of anti-inflammatory IL-10 and inhibitor of proteases TIMP-1 were detected in vCUT. We also showed that vCUT retains endogenous viable cells. The importance of retaining viable cells along with tissue matrix and a plethora of growth factors after tissue preservation has been previously reported in multiple scientific and clinical studies [31,33,35–38]. Accumulated data suggest that preservation of all tissue components is required to retain the full spectrum of biological activities of the fresh tissue [30,31,33,36].

The tissue thickness and vCUT's biomechanical and handling properties make it easy to apply in various surgical procedures. Contrary to most of the currently available synthetic adhesion barriers, vCUT is a viable biological allograft containing all the components needed to serve as an effective adhesion barrier. Collagen- and HA-rich ECM makes vCUT a durable and biodegradable graft. Furthermore, the inhibitory effect on both proliferation and migration of fibroblast, responsible for adhesion formation, is a result of the intrinsic negative charge of HA [11]. Also, positive clinical outcomes of vCUT's surgical use indicate that the tissue allograft has anti-inflammatory properties and supports tissue repair processes [19,21]. The components and properties of vCUT described above suggested its potential benefits for post-surgical adhesion prevention. Hence, the key purpose of this study was to evaluate vCUT as a biological adhesion barrier.

The *in vivo* rabbit model of abdominal adhesion was used to evaluate the effect of vCUT on post-surgical adhesion formation. vCUT's biomechanical properties allowed for ease of handling and suturing onto the abdominal wall. Over the course of the study, the absence of adhesion in all the animals treated with vCUT (with either nonsutured or sutured cecum to abdominal wall) established its effectiveness as an anti-adhesive barrier. Persistence of vCUT at the surgical site allowed control of inflammation and healing of the injured tissue. Furthermore, the rate of degradation of vCUT was gradual and synchronous with the healing of injured tissue. Analysis of tissue sections showed that inflammatory cells were present at the surgical sites, however, these cells are not macrophages (Figs. S2A and B). The abdominal wall and cecum tissue sections were positively stained for iNOS, however, there were no difference between control and vCUT-treated samples (Fig.S2 C, D). Data in the literature suggests that those cells might be smooth muscle cells or T- and B-lymphocytes [39].

There are many different types of adhesion barriers; however, none

of them have all necessary characteristics and properties desired for prevention of post-surgical adhesions [8]. Both natural (hyaluronic acid, chitosan, trehalose, pullulan, phospholipid, and gelatin) and synthetic polymer (expanded polytetrafluoroethylene (ePTFE), and poly [lactic-co-glycolic acid]) (PLGA) materials have been tested for preventing adhesion [11]. Every material has its own drawbacks, which can be divided into three major categories: manufacturing challenges, material oxidation and/or pro-inflammatory properties, or rapid degradation. Some of the materials—such as chitosan, pullulan, and trehalose—have a complex manufacturing process with low yield and high cost. Others, including PLGA and phospholipids, are susceptible to oxidation and trigger inflammation in the host tissue. Biomechanical properties and persistence time post-application are critical characteristics for adhesion barriers. Materials such as gelatin are prone to friction and could cause further tissue damage at the surgical site. Rapid degradation is known drawback of hyaluronic acid, whereas ePTFE is non-biodegradable [11].

Current adhesion barriers used in surgeries primarily function as a physical obstruction separating opposing tissues at the surgical site, but have low potential to control inflammation and support tissue regeneration [8]. A direct comparison of commercially available adhesion barriers in a rat model of adhesion showed that adhesion-free incidence was 20% for Seprafilm (Sanofi-Aventis, Bridgewater, NJ) and Intercoat (FzioMed Inc, San Luis Obispo, California), 3% for SprayGel (Confluent Surgical, Inc., Waltham, MA), and 0% for Adept (Baxter, San Juan, PR) or the control animals without the use of adhesion barrier [40]. Seprafilm is a thin film composed of hyaluronic acid and carboxymethylcellulose that directly applied on the injured tissue to prevent adhesions. Adept, an icodextrin adhesion reduction solution, provides a temporary separation of peritoneal surfaces by hydroflotation. Interceed is a woven fabric adhesion barrier that composed of oxidized regenerated cellulose. Animal studies showed that oxidized regenerated cellulose gelates within approximately 8 h and degrades within 4 days. Seprafilm, Adept, and Interceed are the only three U.S. Food and Drug Administration (FDA)–approved products and are widely used for adhesion prevention [8].

The use of human placental membranes and umbilical cord tissue for a broad variety of surgical applications is well documented in the literature [19,41,42] The anti-inflammatory, antifibrotic and antibacterial properties of placental tissues make them an attractive option for many clinical applications [43–45]. The low immunogenicity of placental tissues allows allogeneic use of placental grafts without matching between donors and recipients [46,47]. Cellular composition of placental membranes and umbilical tissue includes neonatal epithelial cells, fibroblasts and mesenchymal stem cells that are low immunogenic cells [14,48]. Lack of vasculature and nerves within placental membranes and umbilical tissue together with production of anti-inflammatory factors by endogenous placental cells contribute to placental membranes and umbilical tissue low immunogenicity [14,44]. Date above supports that composition and properties of placental tissue allows the use of tissue allografts with viable cells. In our study, using a clinically relevant rabbit abdominal adhesion model, vCUT application led to 100% adhesion-free incidence. vCUT is a human tissue graft, and vCUT is a xenogeneic tissue for rabbits, which is a more severe mismatch in comparison to the allogeneic use. However, even in the xenogeneic settings vCUT prevented post-surgical adhesions in rabbits without triggering an inflammation and rejection. Results of our study support that vCUT, in addition to being a physical barrier, controls inflammation and supports rapid tissue healing. Control of inflammation and rapid tissue healing are critical for adhesion prevention [5,49]. Being a native tissue, the main limitation of vCUT is its sizes. Sizes of vCUT are limited to the size of the umbilical cord tissue, meaning it cannot be scaled up like sizes of synthetic barriers.

In conclusion, this study shows that vCUT reduces post-operative adhesion formation *in vivo*. Future clinical studies confirming the advantages of vCUT as adhesion barrier are further warranted.

## Author contributions

Conceived and designed the experiments: Sandeep Dhall, Jin-Qiang Kuang, Malathi Sathyamoorthy, Alla Danilkovitch. Performed the experiments: Sandeep Dhall, Turhan Coksaygan, Tyler Hoffman, Mathew Moorman, Anne Lerch, Jin-Qiang Kuang, Malathi Sathyamoorthy. Analyzed the data: Sandeep Dhall, Turhan Coksaygan, Tyler Hoffman, Jin-Qiang Kuang, Mathew Moorman, Anne Lerch, Malathi Sathyamoorthy, Alla Danilkovitch. Wrote the manuscript: Sandeep Dhall, Alla Danilkovitch, Malathi Sathyamoorthy.

## Declarations of interest

SD, TH, MM, AL, JQK, MS, and AD are paid employees of Osiris Therapeutics, Inc.

## Acknowledgements

We thank Amy Fried for proofreading the manuscript.

## Appendix A. Supplementary data

Supplementary data to this article can be found online at https://doi.org/10.1016/j.bioactmat.2018.09.002.

## References

[1] D.E. Pittaway, J.F. Daniell, W.S. Maxson, Ovarian surgery in an infertility patient as an indication for a short-interval second-look laparoscopy: a preliminary study, Fertil. Steril. 44 (1985) 611–614, https://doi.org/10.1016/S0015-0282(16)48975-2.

[2] M. Ouaïssi, S. Gaujoux, N. Veyrie, E. Denève, C. Brigand, B. Castel, et al., Post-operative adhesions after digestive surgery: their incidence and prevention: review of the literature, J. Vis. Surg. 149 (2012) e104–e114, https://doi.org/10.1016/j.jviscsurg.2011.11.006.

[3] M.P. Diamond, M.L. Freeman, Clinical implications of postsurgical adhesions, Hum. Reprod. Update 7 (2001) 567–576, https://doi.org/10.1093/humupd/7.6.567.

[4] N. Ray, W.G. Denton, M. Thamer, S.C. Henderson, S. Perry, Abdominal adhesiolysis: inpatient care and expenditures in the United States in 1994, J. Am. Coll. Surg. 186 (1998) 1–9, https://doi.org/10.1016/S1072-7515(97)00127-0.

[5] A.H. Maciver, M. McCall, A.M. James Shapiro, Intra-abdominal adhesions: cellular mechanisms and strategies for prevention, Int. J. Surg. 9 (2011) 589–594, https://doi.org/10.1016/j.ijsu.2011.08.008.

[6] S.V. Pismensky, Z.R. Kalzhanov, M.Y. Eliseeva, I.P. Kosmas, O a Mynbaev, Severe inflammatory reaction induced by peritoneal trauma is the key driving mechanism of postoperative adhesion formation, BMC Surg. 11 (2011) 30, https://doi.org/10.1186/1471-2482-11-30.

[7] N. Sluiter, E. de Cuba, R. Kwakman, G. Kazemier, G. Meijer, E.A. te Velde, Adhesion molecules in peritoneal dissemination: function, prognostic relevance and therapeutic options, Clin. Exp. Metastasis 33 (2016) 401–416, https://doi.org/10.1007/s10585-016-9791-0.

[8] M.P. Diamond, Reduction of postoperative adhesion development, Fertil. Steril. 106 (2016) 994–997, https://doi.org/10.1016/j.fertnstert.2016.08.029 e1.

[9] J. Li, X. Feng, B. Liu, Y. Yu, L. Sun, T. Liu, et al., Polymer materials for prevention of postoperative adhesion, Acta Biomater. 61 (2017) 21–40, https://doi.org/10.1016/J.ACTBIO.2017.08.002.

[10] V.H. Schmitt, A. Mamilos, C. Schmitt, C.N.E. Neitzer-Planck, T.K. Rajab, D. Hollemann, et al., Tissue response to five commercially available peritoneal adhesion barriers-A systematic histological evaluation, J. Biomed. Mater. Res. B Appl. Biomater. 106 (2018) 598–609, https://doi.org/10.1002/jbm.b.33835.

[11] W. Wu, R. Cheng, J. das Neves, J. Tang, J. Xiao, Q. Ni, et al., Advances in biomaterials for preventing tissue adhesion, J. Contr. Release 261 (2017) 318–336, https://doi.org/10.1016/j.jconrel.2017.06.020.

[12] V.L. Ferguson, R.B. Dodson, Bioengineering aspects of the umbilical cord, Eur. J. Obstet. Gynecol. Reprod. Biol. 144 (Suppl 1) (2009) S108–S113, https://doi.org/10.1016/j.ejogrb.2009.02.024.

[13] W. Liao, J. Zhong, J. Yu, J. Xie, Y. Liu, L. Du, et al., Therapeutic benefit of human umbilical cord derived mesenchymal stromal cells in intracerebral hemorrhage rat: implications of anti-inflammation and angiogenesis, Cell. Physiol. Biochem. 24 (2009) 307–316, https://doi.org/10.1159/000233255.

[14] Cho PS, Messina DJ, Hirsh EL, Chi N, Goldman SN, Lo DP, et al. Immunogenicity of Umbilical Cord Tissue–derived Cells n.D. doi:10.1182/blood-2007-03-078774.

[15] B. Weissmann, K. Meyer, The structure of hyalobiuronic acid and of hyaluronic acid from umbilical cord, J. Am. Chem. Soc. 76 (1954) 1753–1757, https://doi.org/10.1021/ja01636a010.

[16] M.L. Weiss, C. Anderson, S. Medicetty, K.B. Seshareddy, R.J. Weiss, I. VanderWerff, et al., Immune properties of human umbilical cord Wharton's jelly-derived cells,

Stem Cell. 26 (2008) 2865–2874, https://doi.org/10.1634/stemcells.2007-1028.
[17] M.L. Weiss, D.L. Troyer, Stem cells in the umbilical cord, Stem Cell Rev. 2 (2006) 155–162 doi:SCR:2:2:155 [pii]\r10.1007/s12015-006-0022-y.
[18] H.-S. Wang, S.-C. Hung, S.-T. Peng, C.-C. Huang, H.-M. Wei, Y.-J. Guo, et al., Mesenchymal stem cells in the Wharton's jelly of the human umbilical cord, Stem Cell. 22 (2004) 1330–1337, https://doi.org/10.1634/stemcells.2004-0013.
[19] K. McGinness, D.H. Kurtz Phelan, Use of viable cryopreserved umbilical tissue for soft tissue defects in patients with gas gangrene: a case series, Wounds a Compend Clin Res Pract 30 (2018) 90–95.
[20] J. Taylor, S. Gearhart, The use of viable cryopreserved placental tissue in the management of a chronic rectovaginal fistula, Ann. R. Coll. Surg. Engl. 99 (2017) e236–e240, https://doi.org/10.1308/rcsann.2017.0157.
[21] J. Ang, C.-K.D. Liou, H.P. Schneider, The role of placental membrane allografts in the surgical treatment of tendinopathies, Clin. Podiatr. Med. Surg. 35 (2018) 311–321, https://doi.org/10.1016/J.CPM.2018.02.004.
[22] O. Makay, D. Isik, V. Erol, C. Yenisey, T. Kose, G. Icoz, et al., Efficacy of simvastatin in reducing postoperative adhesions after thyroidectomy: an experimental study, Acta Chir. Belg. 0 (2016) 1–7, https://doi.org/10.1080/00015458.2016.1242292.
[23] G. Pennati, Biomechanical properties of the human umbilical cord, Biorheology 38 (2001) 355–366.
[24] S. Goktas, J.J. Dmytryk, P.S. McFetridge, Biomechanical behavior of oral soft tissues, J. Periodontol. 82 (2011) 1178–1186, https://doi.org/10.1902/jop.2011.100573.
[25] G.A. Arnold, K.G. Mathews, S. Roe, P. Mente, T. Seaboch, Biomechanical comparison of four soft tissue replacement materials: an in vitro evaluation of single and multilaminate porcine small intestinal submucosa, canine fascia lata, and polypropylene mesh, Vet. Surg. 38 (2009) 834–844, https://doi.org/10.1111/j.1532-950X.2009.00577.x.
[26] S. Shimmura, J. Shimazaki, Y. Ohashi, K. Tsubota, Antiinflammatory effects of amniotic membrane transplantation in ocular surface disorders, Cornea 20 (2001) 408–413.
[27] M. Zare-Bidaki, S. Sadrinia, S. Erfani, E. Afkar, N. Ghanbarzade, Antimicrobial properties of amniotic and chorionic membranes: a comparative study of two human fetal sacs, J. Reproduction Infertil. 18 (2017) 218–224.
[28] N.G. Fairbairn, M.A. Randolph, R.W. Redmond, The clinical applications of human amnion in plastic surgery, J. Plast. Reconstr. Aesthetic Surg. 67 (2014) 662–675, https://doi.org/10.1016/j.bjps.2014.01.031.
[29] A. Silini, O. Parolini, B. Huppertz, I. Lang, Soluble factors of amnion-derived cells in treatment of inflammatory and fibrotic pathologies, Curr. Stem Cell Res. Ther. 8 (2013) 6–14.
[30] Y. Zheng, S. Ji, H. Wu, S. Tian, Y. Zhang, L. Wang, et al., Topical administration of cryopreserved living micronized amnion accelerates wound healing in diabetic mice by modulating local microenvironment, Biomaterials 113 (2017) 56–67, https://doi.org/10.1016/j.biomaterials.2016.10.031.
[31] Y. Duan-Arnold, A. Gyurdieva, A. Johnson, D.A. Jacobstein, A. Danilkovitch, Soluble factors released by endogenous viable cells enhance the antioxidant and chemoattractive activities of cryopreserved amniotic membrane, Adv. Wound Care 4 (2015) 329–338, https://doi.org/10.1089/wound.2015.0637.
[32] Y. Mao, T. Hoffman, A. Singh-Varma, Y. Duan-Arnold, M. Moorman, A. Danilkovitch, et al., Antimicrobial peptides secreted from human cryopreserved viable amniotic membrane contribute to its antibacterial activity, Sci. Rep. 7 (2017) 13722, https://doi.org/10.1038/s41598-017-13310-6.
[33] A. Johnson, A. Gyurdieva, S. Dhall, A. Danilkovitch, Y. Duan-Arnold, Understanding the impact of preservation methods on the integrity and functionality of placental allografts, Ann. Plast. Surg. 00 (2017) 1, https://doi.org/10.1097/SAP.0000000000001101.
[34] A. Fakhari, C. Berkland, Applications and emerging trends of hyaluronic acid in tissue engineering, as a dermal filler and in osteoarthritis treatment, Acta Biomater. 9 (2013) 7081–7092, https://doi.org/10.1016/j.actbio.2013.03.005.
[35] R.G. Frykberg, G.W. Gibbons, J.L. Walters, D.K. Wukich, F.C. Milstein, A prospective, multicentre, open-label, single-arm clinical trial for treatment of chronic complex diabetic foot wounds with exposed tendon and/or bone: positive clinical outcomes of viable cryopreserved human placental membrane, Int. Wound J. 14 (2017) 569–577, https://doi.org/10.1111/iwj.12649.
[36] G.W. Gibbons, Grafix®, a cryopreserved placental membrane, for the treatment of chronic/stalled wounds, Adv. Wound Care 4 (2015) 534–544, https://doi.org/10.1089/wound.2015.0647.
[37] K.M. Raspovic, D.K. Wukich, D.Q. Naiman, L.A. Lavery, R.S. Kirsner, P.J. Kim, et al., Effectiveness of viable cryopreserved placental membranes for management of diabetic foot ulcers in a real world setting, Wound Repair Regen. (2018), https://doi.org/10.1111/wrr.12635.
[38] L.A. Lavery, J. Fulmer, K.A. Shebetka, M. Regulski, D. Vayser, D. Fried, et al., The efficacy and safety of Grafix ® for the treatment of chronic diabetic foot ulcers: results of a multi-centre, controlled, randomised, blinded, clinical trial, Int. Wound J. 11 (2014) 554–560, https://doi.org/10.1111/iwj.12329.
[39] J. Zhang, J. Schmidt, E. Ryschich, M. Mueller-Schilling, H. Schumacher, J.R. Allenberg, Inducible nitric oxide synthase is present in human abdominal aortic aneurysm and promotes oxidative vascular injury, J. Vasc. Surg. 38 (2003) 360–367, https://doi.org/10.1016/S0741-5214(03)00148-4.
[40] T.K. Rajab, M. Wallwiener, C. Planck, C. Brochhausen, B. Kraemer, C.W. Wallwiener, A direct comparison of seprafilm, adept, intercoat, and spraygel for adhesion prophylaxis, J. Surg. Res. 161 (2010) 246–249, https://doi.org/10.1016/j.jss.2008.11.839.
[41] A.C. Mamede, M.J. Carvalho, A.M. Abrantes, M. Laranjo, C.J. Maia, M.F. Botelho, Amniotic membrane: from structure and functions to clinical applications, Cell Tissue Res. 349 (2012) 447–458, https://doi.org/10.1007/s00441-012-1424-6.
[42] M. Karon, Viable umbilical tissue use in laparoscopic myomectomy, Obstet. Gynecol. 131 (2018) 192S, https://doi.org/10.1097/01.AOG.0000533241.41959.96.
[43] N. Kjaergaard, M. Hein, L. Hyttel, R.B. Helmig, H.C. Schønheyder, N. Uldbjerg, et al., Antibacterial properties of human amnion and chorion in vitro, Eur. J. Obstet. Gynecol. Reprod. Biol. 94 (2001) 224–229.
[44] Y. Duan-Arnold, A. Gyurdieva, A. Johnson, T.E. Uveges, D.A. Jacobstein, A. Danilkovitch, Retention of endogenous viable cells enhances the anti-inflammatory activity of cryopreserved amnion, Adv. Wound Care 4 (2015) 523–533, https://doi.org/10.1089/wound.2015.0636.
[45] L.B. Sant'anna, R. Hage, M.A.G. Cardoso, E.A.L. Arisawa, M.M. Cruz, O. Parolini, et al., Antifibrotic effects of human amniotic membrane transplantation in established biliary fibrosis induced in rats, Cell Transplant. 25 (2016) 2245–2257, https://doi.org/10.3727/096368916X692645.
[46] M. Kubo, Y. Sonoda, R. Muramatsu, M. Usui, Immunogenicity of human amniotic membrane in experimental xenotransplantation, Invest. Ophthalmol. Vis. Sci. 42 (2001) 1539–1546.
[47] C.A. Akle, M. Adinolfi, K.I. Welsh, S. Leibowitz, I. McColl, Immunogenicity of human amniotic epithelial cells after transplantation into volunteers, Lancet (London, England) 2 (1981) 1003–1005.
[48] T.Ž. Ramuta, M.E. Kreft, Human amniotic membrane and amniotic membrane–-derived cells: how far are we from their use in regenerative and reconstructive urology? Cell Transplant. 27 (2018) 77–92, https://doi.org/10.1177/0963689717725528.
[49] T. Liakakos, N. Thomakos, P.M. Fine, C. Dervenis, R.L. Young, Peritoneal adhesions: etiology, pathophysiology, and clinical significance - recent advances in prevention and management, Dig. Surg. 18 (2001) 260–273, https://doi.org/10.1159/000050149.